ECOSYSTEMS

United States Forest Disturbance Trends Observed Using Landsat Time Series

Jeffrey G. Masek,[1]* Samuel N. Goward,[2] Robert E. Kennedy,[3,4] Warren B. Cohen,[5] Gretchen G. Moisen,[6] Karen Schleeweis,[2] and Chengquan Huang[2]

[1]Biospheric Sciences Laboratory (Code 618), NASA Goddard Space Flight Center, Greenbelt, Maryland 20771, USA; [2]Department of Geographical Sciences, University of Maryland, College Park, Maryland 20742, USA; [3]Department of Forest Science, Oregon State University, Corvallis, Oregon, USA; [4]Present address: Department of Earth and Environment, Boston University, 685 Commonwealth Ave, Boston, Massachusetts 02215, USA; [5]Pacific Northwest Research Station, USDA Forest Service, 3200 SW Jefferson Way, Corvallis, Oregon 97331, USA; [6]Rocky Mountain Research Station, USDA Forest Service, 4746 S. 1900 E, Ogden, Utah 84403, USA

ABSTRACT

Disturbance events strongly affect the composition, structure, and function of forest ecosystems; however, existing US land management inventories were not designed to monitor disturbance. To begin addressing this gap, the North American Forest Dynamics (NAFD) project has examined a geographic sample of 50 Landsat satellite image time series to assess trends in forest disturbance across the conterminous United States for 1985–2005. The geographic sample design used a probability-based scheme to encompass major forest types and maximize geographic dispersion. For each sample location disturbance was identified in the Landsat series using the Vegetation Change Tracker (VCT) algorithm. The NAFD analysis indicates that, on average, 2.77 Mha y^{-1} of forests were disturbed annually, representing 1.09% y^{-1} of US forestland. These satellite-based national disturbance rates estimates tend to be lower than those derived from land management inventories, reflecting both methodological and definitional differences. In particular, the VCT approach used with a biennial time step has limited sensitivity to low-intensity disturbances. Unlike prior satellite studies, our biennial forest disturbance rates vary by nearly a factor of two between high and low years. High western US disturbance rates were associated with active fire years and insect activity, whereas variability in the east is more strongly related to harvest rates in managed forests. We note that generating a geographic sample based on representing forest type and variability may be problematic because the spatial pattern of disturbance does not necessarily correlate with forest type. We also find that the prevalence of diffuse, non-stand-clearing disturbance in US forests makes the application of a biennial geographic sample problematic. Future satellite-based studies of disturbance at regional and national scales should focus on wall-to-wall analyses with annual time step for improved accuracy.

Key words: forest disturbance; remote sensing; landsat; forest ecology.

INTRODUCTION

Change is ubiquitous in forest ecosystems. Forests experience both seasonality as well as long-term growth cycles that can vary in duration between

50 years and 500 or more years (Waring and Running 2007). These long-term changes are punctuated by mostly short-term disturbances from fire, insects, disease, and harvest which strongly alter the state and functioning of the forest (He and Mlandenoff 1999). Both climate change and the increasing global demand for wood and fiber products are likely to drive increases in forest disturbance rates (Kurz and others 2008; Nepstad and others 2008). These changes in disturbance will alter the water and carbon cycles of forest stands as well as impact the habitat and biodiversity of these ecosystems (Lindenmayer and others 2006; Gardner and others 2009). With respect to the carbon cycle, forest disturbance is now recognized as a major driver of non-fossil-fuels-related terrestrial fluxes to the atmosphere (Running 2008; Amiro and others 2010).

To effectively understand how forest disturbance impacts forest state and functioning, disturbance rates need to be quantified at the spatial grain where human management and natural disturbances occur; typically less than 10 ha (Miller 1978; Cohen and others 2002; Kuemmerle and others 2007; Frolking and others 2009). Furthermore, disturbances need to be quantified at a time step and spatial scale relevant to the affected processes (for example, nationally, annually), and over a temporal period relevant to establishing baselines meaningful to forest policy initiatives (historically, at least as far back as the 1990s) (Böttcher and others 2008; Masek and others 2008; Kennedy and others 2012).

In the United States, the lack of consistent, high-temporal resolution estimates of forest disturbance remains an important gap in efforts to model and manage forest carbon at a national scale (USCCSP 2007; Birdsey and others 2009). The US Forest Service Forest Inventory and Analysis (FIA) Program relies on a network of plots to inventory and monitor forested ecosystems at regional to national scales. Its current annual inventory system (McRoberts and others 2005) closely tracks individual tree mortality and cause of disturbance through remeasurement of inventory plots on a regular cycle (approximately every 5 years in the east, ten in the west). However, until remeasured data are available nationally, consistent forest disturbance estimates cannot be constructed. In addition, FIA is not structured to capture relatively rare disturbance events. Consequently, today's reported US national inventory-based estimates of disturbance area have drawn upon separate databases for the extent of harvest (Smith and others 2009), fire (US Environmental Protection Agency

2011), and insect damage (USDA Forest Service 2010). In some cases, these estimates may be inconsistent. For example, harvest area is derived from a combination of inventory re-measurement data, where available, and harvest activity reports from different National Forests. Insect mortality typically reflects the gross area affected by insects as measured by aerial sketch maps over purposively sampled regions of the country (Johnson and Wittwer 2008), although recent efforts have begun to convert these maps into true mortality estimates (Meddens and others 2012).

Satellite observations may provide a more consistent means for assessing disturbance. Previous studies estimating national and global forest disturbance patterns have used coarse-resolution (250 m–1 km) satellite imagery (NOAA AVHRR and NASA EOS MODIS) (Potter and others 2005; Mildrexler and others 2009; Potapov and others 2009). Although suitable for detection of large-area disturbances such as fire and large-scale clearcuts, coarse-resolution imagery is less capable of detecting forest management activities than finer-grained observations from satellites such as Landsat (Skole and Tucker 1993; Tucker and Townshend 2000; Bucha and Stibig 2008; Wulder and others 2008; Potapov and others 2009). Studies that use imagery of finer spatial grain have either mapped at too coarse a temporal grain to detect short-term changes in forest disturbance rate (Masek and others 2008; Hansen and others 2010) or have focused only a single type of forest disturbance (for example fire mapping from the Monitoring Trends in Burn Severity project, MTBS, Eidenshink and others 2007). The need to overcome limitations inherent in these previous or ongoing ground-based and satellite-based disturbance analysis efforts has motivated the development of the North American Forest Dynamics (NAFD) project (Goward and others 2008), a core project of the North American Carbon Program (Wofsy and Harris 2002).

The study reported here was derived from the first two phases of NAFD, which employed a geographic sample of Landsat observations at a relatively high-temporal frequency (approximately annual time step) over a 20-year period to characterize the dynamics of recent US forest disturbance history. A sampling approach was selected due to the high cost of individual Landsat images (~$600) when this study was initiated (2005) and the fact that an annual, wall-to-wall analysis would involve over 9,000 such images covering the 442 individual scenes over the conterminous

US.[1] We selected a sample of 50 scenes and for each we assembled a time series of cloud-minimized, seasonally consistent imagery. The time series of each pixel in a given image stack was analyzed using the Vegetation Change Tracker (VCT) algorithm to detect disturbances (Huang and others 2010a).

In this study, forest disturbance was defined as any event that caused either substantial mortality or leaf-area reduction within a forest stand, including management activities such as harvest and thinning. As described more fully in the ''Methods'' section, the VCT approach captures most rapid stand-clearing events (including clearcut harvests and fire), as well as many non-stand-clearing events (partial harvest, thinning, storm damage, insect damage). However, gradual declines in live biomass that occurred over several years (for example, due to drought or disease) were mostly not captured. The approach also did not distinguish between disturbance (mortality followed by recovery) and permanent conversion of land cover. Thus, our definition of disturbance corresponds most closely to *gross forest cover loss* (Hansen and others 2010). Although knowing the causal agent of disturbance is extremely important for understanding specific impacts on ecosystems, this study has not attempted to assign an agent to each disturbed patch. Instead, we focus on overall ''turnover'' of live forest area across the county.

Our central objective was to estimate annual rates of forest disturbance across the conterminous US. Accomplishing this required the development and application of novel methods to: (i) select a probability-based sample of 50 scenes while satisfying diverse analytical criteria; (ii) apply an automated change-detection algorithm to identify forest disturbance across a Landsat image time series for each scene, and (iii) assign estimates of sampling errors associated with this disturbance mapping.

METHODS

Sample Design

Our sample design followed the rules of probability-based sampling (Särndal and others 1992), where each scene had a known, non-zero, positive probability of inclusion in the sample, and the set of possible samples was finite and known. This

approach allowed for design-based estimation and for preferential inclusion of scenes with greater land or forest area (Gallego 2005), an important consideration given the effort and cost involved in the analyses and the central goal of characterizing forest disturbance. This approach also allowed for inclusion of other important characteristics: spatial dispersal of scenes to minimize autocorrelation, assurance that all major forest types were included as forest disturbance and recovery dynamics are largely type-specific, and the ability to leverage work already completed at a handful of ''targeted'' scenes available from related projects (for example, Masek and Collatz 2006; Eidenshink and others 2007).

Fundamental to our sampling design was the choice of sample unit (geographic area of a single sample scene) and sample frame (the population of sample scenes covering the conterminous US). Because adjacent WRS-2 Landsat frames overlap, the sample frame was modified such that each scene was trimmed to include only the unique, non-overlapping area it contained. This ensured that each sample scene was unique, and simplified the use of population statistics. Hereafter, our reference to sample scenes implies the non-overlapping portion of scenes produced by this process.

As a first step in assuring that scenes with greater forest cover were preferentially selected as part of the sample, several scenes with extremely low forest cover were culled from the sample frame. This was accomplished by ranking each sample by total forest area (based on a US forest type map developed by Ruefenacht and others 2008) from low to high, and eliminating all ranked scenes for which the total forest area was below 2% of the cumulative forest area across all scenes in the frame.

We divided the culled sampling frame into two strata: eastern and western. This division reflects that fact that at a gross scale eastern and western US forests are fundamentally different ecologically and in terms of how they are managed, both of which could greatly affect disturbance and recovery dynamics. To accomplish this division all Landsat scenes in WRS-2 Path 31 or greater were declared western and all scenes in Path 30 or less were declared eastern. All further steps were executed separately for each stratum.

For each stratum, samples were drawn from randomly ordered lists of scenes. Rather than creating a single list, a set of v (=100,000) scene lists were created, each with a different random ordering, and the final sample was chosen by randomly selecting one list from the set of lists that met our preferential criteria: geographic scene dispersion, maximizing total forest area, forest type diversity, and inclusion of targeted scenes where we have

---

[1] In this article, we use the term ''scene'' to refer to the nominal geographic area of a particular Landsat Worldwide Reference System (WRS-2 path/row). The actual Landsat acquisitions from specific dates for that area are termed ''images'' (see Strahler and others 1986).

Table 1.   Ordered List of the Sample Scenes Chosen in Each Stratum (Eastern, Western) with Probability of Inclusion

Order	Eastern stratum		Western stratum	
	WRS-2 path/row	Probability of inclusion (π)	WRS-2 path/row	Probability of inclusion (π)
1	21/37	0.138	37/34	0.117
2	27/38	0.130	35/34	0.234
3	22/28	0.154	34/37	0.183
4	18/35	0.146	37/32	0.157
5	25/29	0.118	47/28	0.183
6	17/31	0.142	36/37	0.213
7	19/39	0.126	41/32	0.213
8	16/36	0.177	43/33	0.198
9	26/36	0.157	41/29	0.162
10	12/31	0.122	35/32	0.112
11	21/39	0.134	45/29	0.173
12	12/27	0.146	44/26	0.137
13	26/34	0.142	42/35	0.137
14	24/37	0.114	42/28	0.208
15	21/30	0.197	44/29	0.168
16	23/35	0.130	46/32	0.188
17	26/37	0.114	46/31	0.223
18	14/31	0.142	42/29	0.157
19	16/35	0.142	46/30	0.178
20	16/41	0.169	47/27	0.157
21	23/28	0.165	48/27	0.168
22	20/33	0.154	40/37	0.152
23	15/31	0.122	34/34	0.193
24	27/27	0.087	33/30	0.183
25	19/36	0.122	45/30	0.152

important experience. This provides two important benefits. First, for any given set of lists, every scene's probability of inclusion (π) in the sample could be calculated directly as its proportional occurrence in the first n scenes across all lists in the set. Second, because the probability of inclusion was calculated directly, it was possible to further cull the set of lists from the frame to remove those whose first n scenes, taken together, did not meet our preferential selection as described above.

The final sample was chosen by randomly selecting one list per stratum from the final culled list in each stratum. The sample size (n) for each stratum was 12 (eastern) and 11 (western), given that the sample design and list selection was executed during the first phase of the project when only 23 scenes were under consideration. For each sample scene π was calculated as the number of times the sample appeared among the first n scenes in the set of v lists, divided by v. During the second phase of the project, when we added the next sequential 13 (eastern) and 14 (western) samples from the two ordered lists new π were calculated

for each sample by increasing n to 25 for each stratum. The final set of 50 samples is listed along with their probabilities of inclusion in Table 1, and a map illustrating the spatial distribution of the samples is shown in Figure 1. In addition, a comparison of the forest type map used for sample selection with the forest types represented in our samples demonstrates that the design was effective at capturing the diversity of US forest types in the sample frame (Ruefenacht and others 2008) (Figure 2).

Deriving the Scene-Level Disturbance Products

The creation of scene-level NAFD disturbance products has been described in detail previously (Huang and others 2009, 2010a, b; Thomas and others 2011). Here, we briefly summarize the steps required to map disturbance within each Landsat sample scene and then describe the quality of the products in terms of severity and types of disturbance detected.
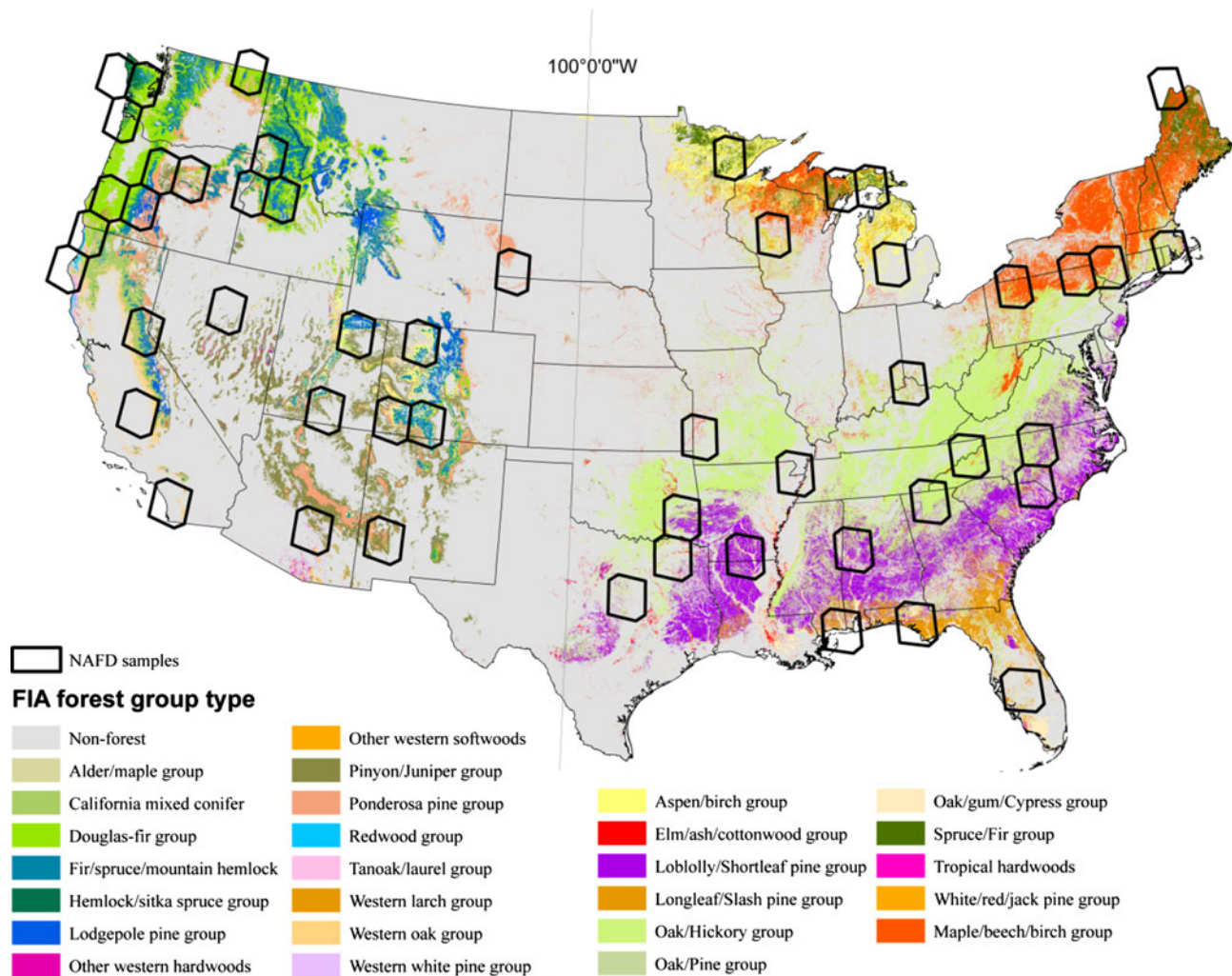
Figure 1. NAFD sample scenes (unique, non-overlapping scene areas) overlaid on the US forest type map (Ruefenacht and others 2008).

At each of the 50 sample locations, a Landsat image time series was constructed consisting of one image during the growing season (leaf-on conditions) for (initially) a target of every other year, between 1985 and 2005. Although biennial image acquisition was the initial targeted frequency, we were able to augment most image stacks with higher temporal frequency (that is, mean intervals less than 2 years). To optimize detection of change, images were chosen based on cloud cover and seasonality, with no attempt to synchronize skipped years in different stacks. Leaf-on seasonality required acquisition dates between June and September for most of the United States, although the range was extended to include May and October in the southern states.

Each image stack was processed to maintain the highest radiometric and geometric standards

(Huang and others 2009). Imagery was obtained as standard L1T (orthorectified at-sensor radiance) files from USGS EROS, and the latest version of the appropriate sensor calibration parameter set was applied. Geometric registration was checked and (as necessary) corrected by automated selection of image tie points and orthorectification (Huang and others 2009). The images were then converted to surface reflectance using the LEDAPS atmospheric correction package (Vermote and others 1997; Masek and others 2006) and assembled into a time series stack clipped to a common geographic extent.

Finally, water, cloud, and cloud shadow were identified and masked in each image. Water was mapped through a combination of decreasing reflectance with wavelength and low NDVI value (Huang and others 2010a). Clouds were mapped using a set of visible/top-of-atmosphere temperature
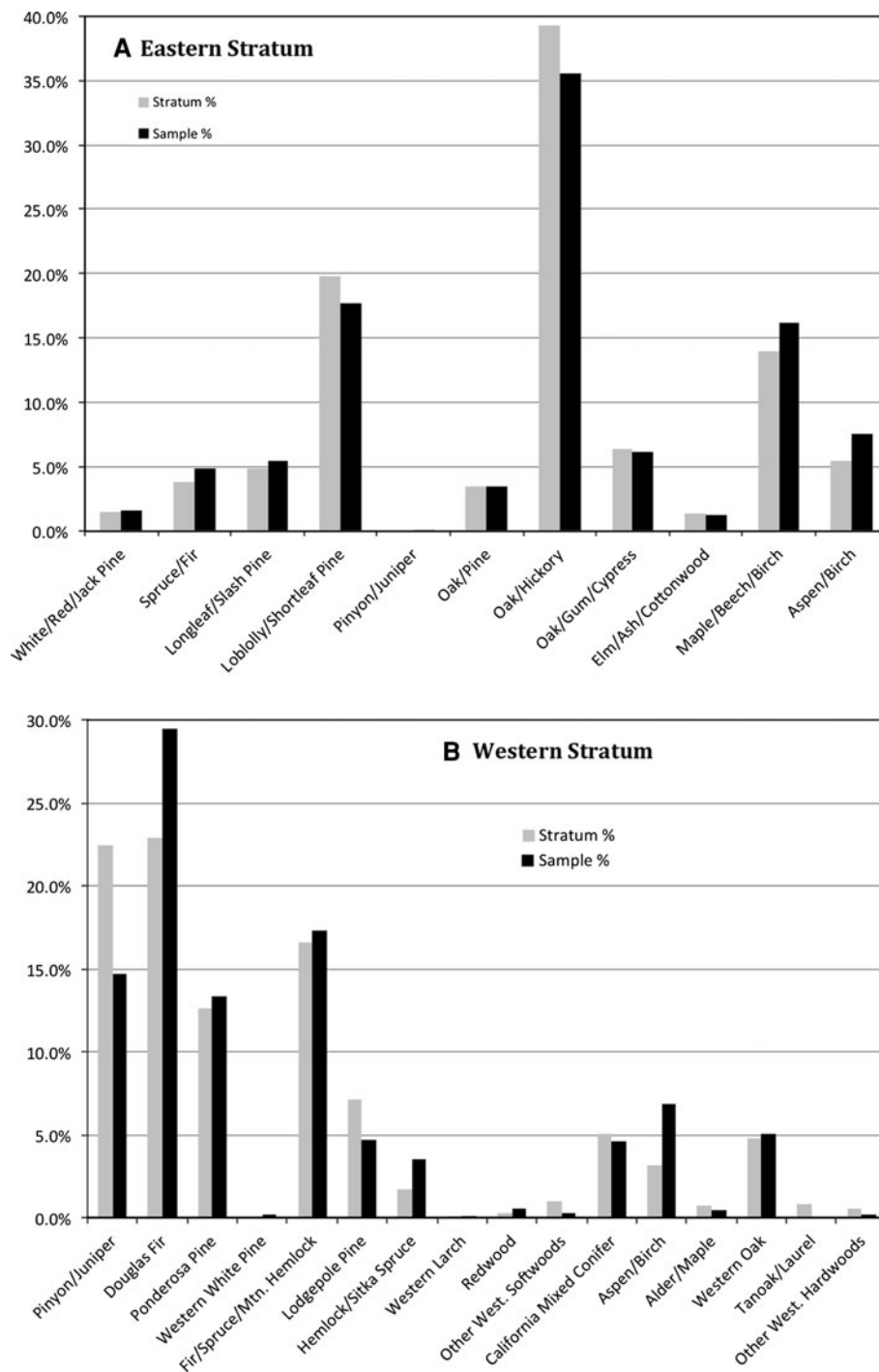
Figure 2. Fraction of forest types captured by the NAFD sample for the **A** eastern and **B** western strata (*gray bars*) compared to the actual area of each type from the map of Ruefenacht and others (2008) (*black bars*).

relationships (Huang and others 2010b). Residual cloud contamination not identified in this step was also isolated as single-year "outliers" in the VCT forest disturbance analysis discussed below, and removed.

Forest disturbances were mapped from the Landsat time series stacks using the VCT algorithm (Huang and others 2010a). The algorithm used an automated approach to select forest training sam-

ples in each Landsat image and then calculated the distance in spectral space between each image pixel and the centroid of the forest training population (Huang and others 2010a). Pixels close to the centroid of the forest population in the spectral space across the entire time period of record were classified as persistent forest for the entire observing period. Forest disturbance year for a given pixel was identified when that pixel's spectral properties
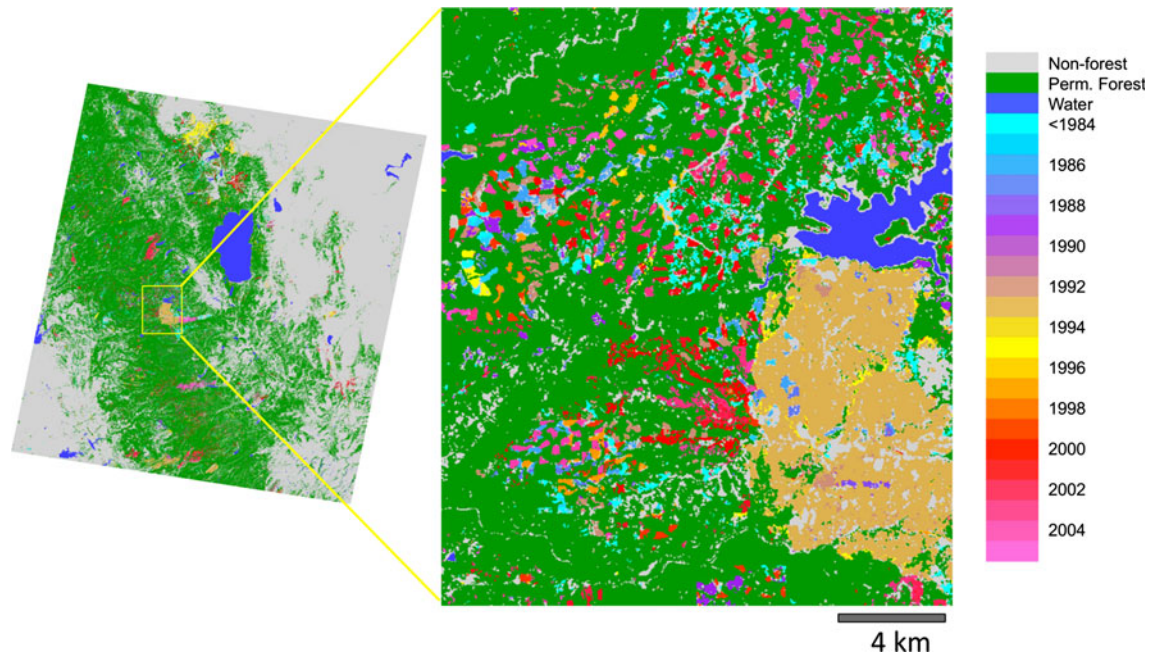
Figure 3. Example of vegetation change tracker (VCT) algorithm output for Landsat WRS-2 path 43 row 33 (Sierra Nevada, California). The VCT uses per-pixel annual Landsat time series to generate maps with classes for permanent forest, non-forest, and disturbance occurring in each year. Disturbed patches are color-coded by year of disturbance. Lake Tahoe is depicted as the *blue area* in the north-center of the full scene. *Zoomed image* Small patches of harvest as well as the large burn scar of the 1992 Cleveland fire.

exceeded an expected range of spectral deviation scores for at least two subsequent sequential time steps. The algorithm generated maps with classes for persistent non-forest, persistent forest, water, and the year of disturbance (Figure 3).

These maps were filtered in both the spatial and the temporal domains. Filtering was necessary to reduce false positive detections (''speckle'') caused by residual image misregistration (Townshend and others 2000; Knight and Lunetta 2003). Disturbance pixel groups that were adjacent in space and time (that is, within one time period of each other) were identified. A majority filter was applied to achieve a minimum mapping (MMU) of 0.16 ha (two pixels) for static persistent forest and non-forest classes and 0.32 ha (4 pixels) for disturbance classes. Disturbance pixels in groups smaller than the MMU were converted to a majority class using decision rules in conjunction with a mode filter in the local 3 × 3 pixel neighborhood. Majority filtering typically reduced per-scene disturbed area by about 20%.

Per-scene Disturbance Product Quality

Two approaches were used to describe disturbance product quality. First, six scenes representative of

a range of forest and disturbance classes were selected to evaluate VCT performance (Thomas and others 2011). These locations included a variety of disturbance types, including forest fire, harvest, thinning, land-use conversion, and both storm and insect damage. The maps derived from VCT were compared to estimates determined independently using expert visual interpretation of Landsat and high-resolution satellite imagery. Because no field-based datasets exist that match the temporal density and spatial detail of the Landsat observation, a field-based validation was not undertaken (Cohen and others 2010). Rather, trained interpreters, using established photo-interpretation guidelines, visually evaluated the Landsat TM imagery in tandem with high-resolution digital imagery such as that available on the Google Earth. The Google imagery was used to aid determination of final land cover/use and to provide geographic context, whereas the determination of forest change came from visual interpretation of the Landsat TM imagery. The interpreters labeled change and no-change conditions using knowledge of both the land spectral properties and the spatial context of the landscape. This process was conducted at over random 600 points for each of the six validation scenes, with the points stratified by disturbance

class (that is, year of disturbance mapped). For each scene, accuracy metrics of the VCT map were calculated by comparing that map with the visual interpretation results.

The results yielded overall per-scene accuracies of 77–86% and kappa values of 0.67–0.76 (Thomas and others 2011). Considering only the forest change classes, omission and commission errors varied widely due to small sample sizes for individual year classes. Forest change users' accuracies (100% − commission error%) averaged 55–79% among the six scenes, although these accuracies increased by approximately 9% if the VCT year of disturbance was allowed to be within 1 year of the reference assignment. In general, omission errors were higher than commission errors. As a result, disturbance rates calculated from VCT map products were biased, underestimating total disturbance by an average of 24% across all validation sites. Omission errors mainly reflected the limitations of biennial sampling for capturing subtle disturbances (for example, mechanical thinning), effects of seasonality within the image time series, and limitations of the VCT algorithm for mapping gradual, multi-year declines in forest health (that is, stress) and change in the sparse forests of the western US.

The specific type of disturbance was a lesser control on accuracy compared to the severity of disturbance, defined as the fraction of tree cover killed within the 0.32 ha MMU. Both natural and anthropogenic stand-clearing disturbances (principally clear-cut harvest, severe fires, and major storm events) could be detected with high accuracy (75–85% detection accuracy), whereas non-stand-clearing disturbances (including thinning, understory burns, and insect defoliation events) were only detected with 38% accuracy (Thomas and others 2011). It should be noted that this latter figure increased to 60% accuracy if the allowable temporal window was relaxed to ±1 year.

In a second subsequent analysis (unpublished data), we used the TimeSync Landsat times series validation tool (Cohen and others 2010) to better describe omission errors in terms of disturbance severity and type. TimeSync is a software environment to support visualization and interpretation of Landsat time series data. It includes simultaneous display of multitemporal Landsat image subsets, per-pixel Landsat spectral time series, and temporal snapshots of high-resolution imagery available in Google Earth. Interpreters can use the TimeSync environment to assign land cover, land use, and change labels to per-pixel trajectories, and then store this information in an online database. For this analysis, we examined

150 plots randomly located within each of nine of the 50 sample scenes. Three severity classes were defined based on the percent of canopy removed or killed by disturbance (<34, 34–67, and >67%). In the high and medium severity classes, 10 and 23% omission rates were observed. In contrast, the omission rate for the low severity disturbance class was 68%. However, although omissions errors were linked to disturbance intensity, they were not uniform across disturbance type, indicating an interaction between severity and causal agent in terms of omission rates.

For the three dominant types, harvest, fire and stress, omission rates in the low severity class were 76, 38, and 85%, respectively. This suggests that fire is the most likely and stress the least likely type of disturbance detected by VCT, with clear-cut harvest much more likely to be detected than selective harvest. For this analysis, we defined stress as any observation of a spectral trend in the direction of disturbance that involved the loss of leaf area (or death) of live woody vegetation and was supported by observations within Google Earth. To be declared stress, the spectral trend had to be multi-year (typically 5 or more years). We assumed that the large majority of such observations were associated with insect and disease activity (largely in conifer forests), recognizing that some observations were associated more directly with prolonged drought (for example, in pinyon-juniper and shrublands). We could not observe seasonal losses of foliage associated with insects that would subsequently recover to full or near-full leaf area the following year (for example, in eastern deciduous forests). The TimeSync analysis supported the initial observation that omission error was greater than commission error and that omission error was more strongly associated with disturbance severity than type.

Estimation of Area Disturbance Rates and Uncertainty

To estimate disturbance rates, we first derived annual totals of disturbed area for each of the 50 NAFD sample scenes by interpolating across missing years of data within the scene. This was accomplished by allocating mapped disturbance from any multi-year period evenly to each year within that period. For example, if the 1992 image was missing from the time series, and 10,000 ha of disturbance was mapped during the 1991–1993 period, 5000 ha of disturbance would be allocated each to 1992 and 1993. Gaps in the image time series were asynchronous among samples, and

more than half of the samples in each stratum provided data for any given year. Total forest area was also calculated for each scene by summing across three mapped classes: persistent forest, disturbed forest, and forest recovering from a pre-time series disturbance (Huang and others 2010a).

From our samples, total disturbed area per year and total forest area were estimated for the two strata using the generalized Horvitz–Thompson (1952) estimator for unequal-probability designs:

$$A = \sum_{i=1}^{n} \frac{y_i}{\pi_i}, \tag{1}$$

where A is the unbiased estimate of either forest area or disturbed area for a given year, y_i is the forest or disturbance area for the ith sample in that year, and π_i is the probability of inclusion for the ith sample. Proportional forest disturbance rate by stratum was calculated by dividing this total by the estimated total forest area in the stratum. Estimation of variance was achieved using the conservative collapsed stratum variance method (Cochran 1977).

RESULTS

Per-scene Disturbance Rates

Raw, per-scene forest area and disturbance rates for each of the 50 samples showed significant geographic variability (Figure 4). Disturbance rates in the southern United States and Pacific Northwest were consistently high, both in terms of absolute area and fraction of mapped forest cover affected. Samples from the Carolinas, the Gulf Coast, and northern Louisiana exhibited fractional disturbance rates in the range of 1.5–2.0% y^{-1}. Absolute and

fractional disturbance rates in the northeast were considerably lower ($<0.5\%$ y^{-1}). Although the absolute area of disturbance in the interior (mountain) west was low, the forest cover base in these locations is limited and generally confined to mountain environments, and corresponding fractional disturbance rates were quite variable.

Eastern versus Western US Disturbance

Having selected independent sample sets for the eastern and western United States, disturbance rates and variances were estimated separately for each stratum (Figure 5). We found similar average disturbance rates (1.10 and 1.05% y^{-1}, respectively) for eastern and western forests, and significant interannual variability in disturbance rates within each of the stratum. However, the annual rates of disturbance were asynchronous in the two strata. Although both strata showed decreases in disturbance rate from the late 1980s to the early 1990s, thereafter the trajectories within the two regions diverged, with disturbance rates peaking in the east in the late 1990s and in the west in the early 2000s.

The national sampling approach does not support disaggregating the results to finer geographic areas because the probability of inclusion for each sample scene was calculated assuming two strata. Thus, there is no way to produce a subregional area estimate other than simple averaging (that is, assumed equal probability of inclusion). With that caveat, we can calculate such "apparent" disturbance rates for smaller groups of scenes to interrogate regional patterns. Disturbance rates were explored independently for groups of scenes within the northern and southern subregions of the eastern stratum, and for groups of scenes within the
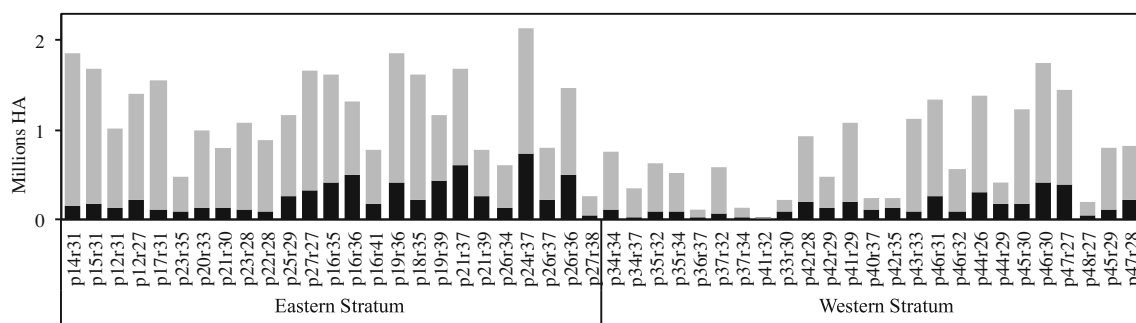

Figure 4. Per-scene results of the NAFD disturbance analysis. The overall length of the bar shows total NAFD derived forest land area for the WRS-2 sample location (*x* axis). The *black portion* of the *bar* is equal to the area of forest mapped as disturbed during 1985–2005. Note that samples along coastlines show low forest area due to the large proportion of water that falls within the samples footprint.
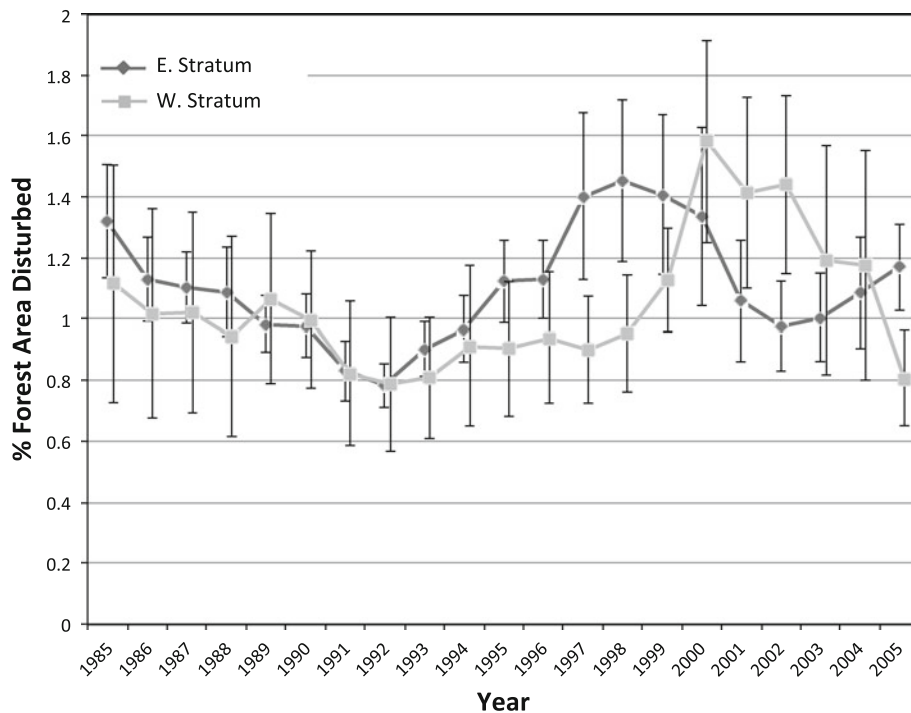
Figure 5. Disturbance rates and uncertainty estimates calculated separately for the eastern (*dark gray*) and western (*light gray*) strata. *Error bars* represent sampling error ($\pm 1\sigma$) and western points are offset by 0.2 years for clarity.

intermountain and coastal subregions of the western stratum (Figure 6). These boundaries correspond to the US Forest Service FIA regions. In the western US, disturbance rates in the intermountain west were generally lower than the coastal region, with the difference becoming more pronounced in the late-1990s. In the eastern US, the northern and southern subregions show markedly different temporal patterns. Although the northern subregion indicates a stable, low rate of disturbance, disturbance rates in the southeast are much higher and vary significantly on 5- to 10-year timescales. It should be noted, however, that because the results for individual subregions do not come from the full per-stratum sample, variances cannot be calculated for these rates. Thus, although the temporal patterns can be broadly interpreted, their statistical significance is uncertain.

National Disturbance Rates

Aggregating the results from the eastern and western strata gives an estimate of national forest disturbance rates since 1985 (Figure 7). We find that an average of 2.77 $y^{-1} \pm 0.36$ Mha (1 σ) of US forestland was disturbed each year during the 1985–2005 period. This figure corresponds to a fractional disturbance rate of 1.09% forestland per year. The net underestimation bias (see ''Per-scene Disturbance Product Quality'' section) suggests that the VCT algorithm missed about 24% of actual

disturbance that can be detected visually within the Landsat imagery. Adjusting the NAFD results for this underestimation bias would increase the national disturbance rate from 2.77 Mha y^{-1} (1.09% forestland y^{-1}) to 3.63 Mha y^{-1} (1.42% forestland y^{-1}).

Unlike studies that report only average disturbance rate over multi-year periods our results suggest that forest disturbance rate can change rapidly across large regions (Figure 7). The time series of national disturbance varies about the mean value, from a low of 0.8% of US forest area in 1992 to a high of 1.4% in 2000. In general, values during the early 1990s were consistently lower than average, whereas values in the late 1990s were consistently higher. The uncertainty bounds based only on sampling error are less than the magnitude of the interannual variability, suggesting that these swings in disturbance rates at the national scale are ''real'' and not simply artifacts of the sampling. However, some caution must be taken given that only sampling errors are shown in Figures 5 and 7; inclusion of measurement errors would increase estimated error and reduce confidence in the estimates of interannual variability.

US Forest Area

Total forest area for the conterminous US was also calculated from the NAFD results, estimated as the sum of permanent (undisturbed) forest and all
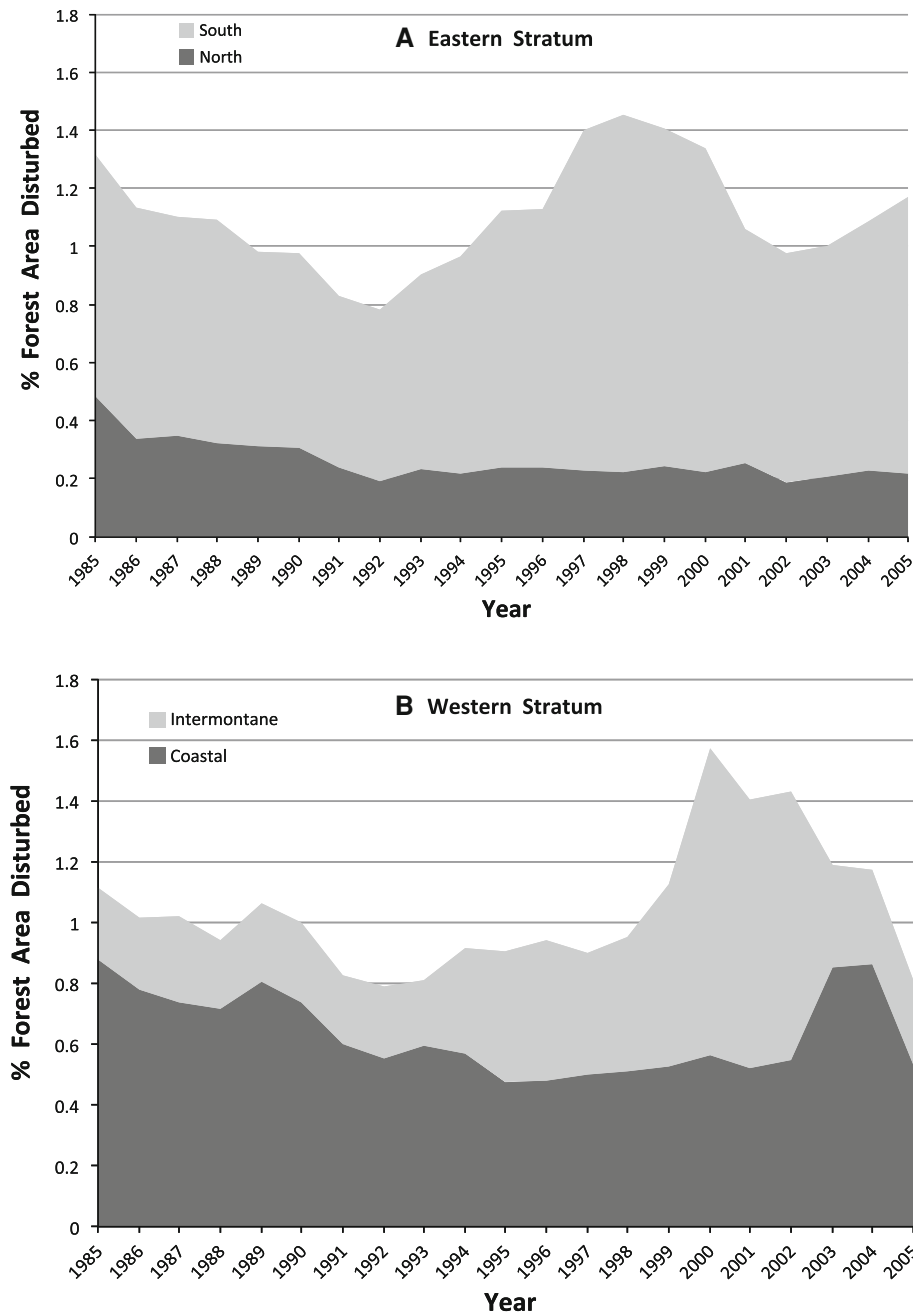
Figure 6. Disturbance rates (%forest change per year) calculated for **A** the south and north subregions of the eastern stratum and **B** the intermountain and coastal subregions of the western stratum. The *thickness* of each *shaded area* gives the disturbance for that subregion, such that the *upper surface* gives the total disturbed area for each stratum.

annual disturbance classes within the VCT classification. The estimated total forest areas for the eastern and western strata were 182×10^6 and 74×10^6 ha, respectively, for a total estimate of 255×10^6 ha. The US Forest Service reported areas of 157×10^6 and 96×10^6 ha for eastern and western forestland in 2007, respectively (Smith and others 2009). Thus, although the NAFD national forest area corresponds closely to the US Forest Service national estimate of 253×10^6 ha for forestland in the conterminous US, the per-stratum areas are somewhat different.

DISCUSSION

National Disturbance Rates

The results presented here represent the first satellite-based estimates of yearly forest disturbance for the conterminous United States. From our geographic sample, we have estimated that, on average, 1.09% of US forestland was affected by disturbances each year during the 1985–2005 epoch. It should be noted, however, that our sample was primarily based on representing forest type, and the geographic distribution of disturbances
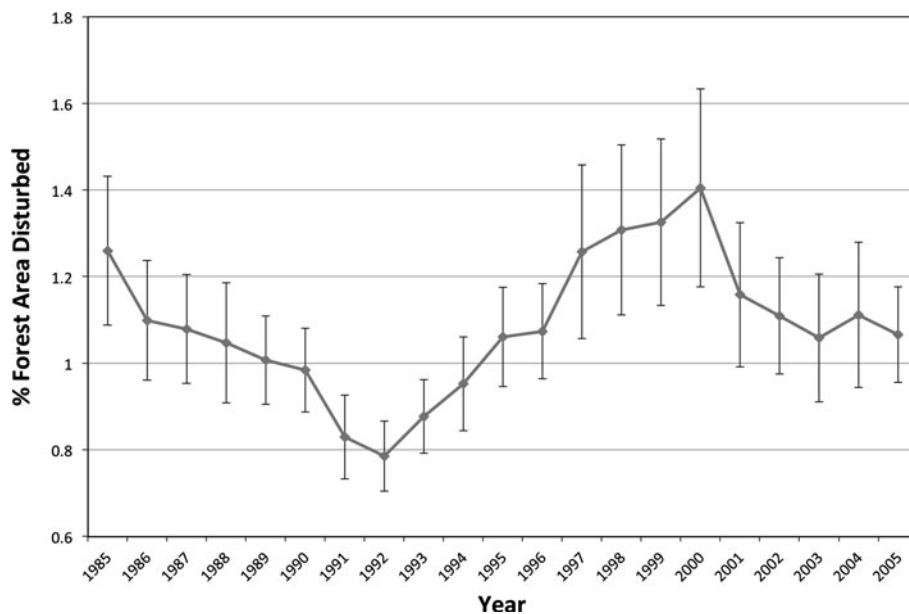
Figure 7. NAFD national disturbance rates obtained by combining results for the eastern and western strata, calculated by year (% of conterminous forest area disturbed per year). *Error bars* Sampling error ($\pm 1\sigma$).

does not necessarily correspond to that of forest types. Therefore, there is some additional uncertainty in the national rates not captured by the estimate of sampling error.

It is of interest to compare our results to data from US land management inventories, as well as previous remote sensing studies (Table 2). As noted in the "Introduction," there is no single database from the US forest inventory that tracks the area of forest disturbance. However, there are independent reports for the area of harvest (including area affected by partial harvest) (Smith and others 2009), the area affected by forest fire (EPA 2011), and the forest area affected by insect mortality (USDA Forest Service 2010). The age distribution of US forests reported in the FIA can also be converted to an average stand-clearing disturbance rate assuming that all forestland area younger than 20 years experienced a stand-clearing disturbance event during the last 20 years. This calculation implicitly excludes non-stand-clearing events that would reduce stand biomass but not necessarily alter the FIA age assignment.

Previous remote sensing estimates of US forest disturbance are given in Masek and others (2008) based on a 10-year (1990–2000) wall-to-wall analysis of Landsat imagery, and Hansen and others (2010) based on 500-m resolution MODIS imagery for the 2000–2005 time period. Like the NAFD sample, these estimates represent gross forest cover loss; that is they include both losses due to disturbance (but that will return to forest cover) as well as losses due to permanent forest conversion (deforestation). However, the rate of deforestation in the US is relatively low compared to the turn-over due to harvest and other forms of disturbance (Smith and others 2009). Drummond and Loveland (2010) also used Landsat data in 5- to 7-year epochs to estimate land-cover transitions in the eastern US. They found gross forest conversion (which includes harvest and permanent conversion) of 0.34 Mha y^{-1}, although this cannot be directly related to the NAFD eastern stratum because the Drummond and Loveland (2010) study area only included areas east of the Mississippi and Ohio Rivers.

Comparing these studies suggests a general consistency among the satellite-based disturbance estimates (Table 2). The NAFD national results are higher than those of either Masek and others (2008) or Hansen and others (2010), presumably reflecting an improved ability to identify subtle disturbance signals when using finer spatial resolution data (compared to MODIS) and shorter mapping intervals (compared to the decadal Landsat study). The NAFD rates are also higher than those calculated from the FIA forestland age distribution, suggesting that the NAFD results are identifying a significant amount of partial harvest (that is, thinning) that would not be severe enough to reset the FIA stand age. This is corroborated by the TimeSync assessment that indicated most moderate and some low severity disturbances were detected.

All of the satellite-based estimates are considerably lower than the rates obtained by summing the inventory-based estimates of forest harvest, fire, and insect mortality. The total area of disturbance obtained from the inventory reports is about 8.1 Mha y^{-1}, with 4.3 Mha y^{-1} attributable to

Table 2. Comparisons of Estimated US Disturbance Rate from this Study with Previous Satellite and Inventory-based Studies

Category	Source	Period of record	Extent	Method/source	Type	Forest area disturbed (Mha y^{-1})
Remote sensing	Masek and others (2008)	1990–2000	Conterminous US	Wall-to-wall mapping with two dates of Landsat imagery	Observed, stand-replacing disturbances	1.97
	Hansen and others (2010)	2000–2005	US (incl. AK and HI)	Sample-based mapping using two dates of Landsat imagery and MODIS	Observed disturbance	2.5
	This study	1985–2005	Conterminous US	Sample-based mapping with dense time series	Observed disturbance	2.77 (±0.76)
					Adjusted disturbance[1]	3.63
FIA age		1988–2008	Conterminous US	Annualized area of forests <20 years in age	Stand-replacing disturbance	2.2
Inventory	Smith and others (2009)	2001–2005	Conterminous US	Remeasured inventory plots in east, National Forest activity reports in west	Clearcut and partial harvest	4.34
	US Environmental Protection Agency (2011)	1990–2005	Conterminous US		Forest fire	1.01
	USDA Forest Service (2010)	Late-2000s	US (incl. AK, HI)	Aerial Detection Survey (ADS)	Area affected by insect disturbance	2.74
	Meddens and others (2012)	1997–2010	Western US	ADS calibrated to area of mortality	Beetle mortality	0.38

[1]Adjusted disturbance includes lower-intensity forest disturbance and is based on application of the bias omission factor as described in ''National disturbance rates'' section.
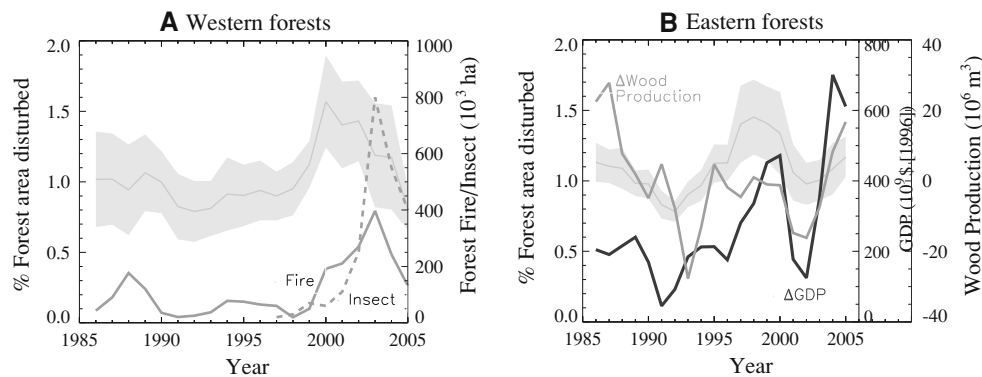
Figure 8. Temporal patterns of forest disturbance rates compared to factors expected to influence those rates for the western (**A**) and eastern (**B**) US. Wood production and GDP rates refer to year-to-year changes in 2-year running average national estimates (Howard 2007). Fires are areal estimates of forest fire disturbance alone for the western US obtained from the Monitoring Trends in Burn Severity (MTBS) project (mtbs.gov). *Insects* represent the upper bound of beetle-associated mortality area (Meddens and others 2012).

harvest activity alone (Table 2). There are two likely explanations for the discrepancy. First, the inventory data generally record the area affected by a type of disturbance rather than the actual area of forest disturbed. For example, the insect mortality estimate is based on the area enclosed by areal sketch map polygons, whereas only a fraction of the stands within those polygons have succumbed (Johnson and Wittwer 2008). Meddens and others (2012) assessed the actual tree mortality area within USFS Aerial Detection Survey polygons for beetle outbreaks in the western US, and estimated up to 380,000 ha y^{-1} of actual tree mortality averaged for the 1997–2010 period. Similarly, the area considered affected by partial harvest (for example, selective cutting or strip cuts) may be less than the actual area cleared. In contrast, the satellite-based results offer the potential for a more exact estimate of disturbed crown area.

However, some of the discrepancy also likely reflects limitations of the current NAFD methodology. The methods described here are sensitive to most severe and moderate disturbances, but commonly miss events that kill a small fraction of trees within the stand or disturbances that emerge gradually (such as drought or insect mortality). In addition, the accuracy of the VCT change detection was hampered by occasional inconsistencies in the acquisition date of images within the time series. Using the bias-adjusted figure derived from Thomas and others (2011) of 3.63 Mha y^{-1} (1.42% forestland y^{-1}) brings the satellite-based disturbance estimates closer to the inventory figure. Finally, there remains the possibility that the NAFD

sampling approach introduced some bias into the results compared to geographically comprehensive estimates from forest inventories.

Interannual Variability

The NAFD results also suggest significant interannual changes in disturbance rates. However, our national estimates integrate across the many factors (forest policy and management, fire ignition, local economic conditions, land ownership) that determine forest disturbance rates when viewed at the local or regional scales. We do know that a primary causal factor in disturbance rates is forest management, specifically harvest. The quantity of timber harvested is a function of societal, economic, and political processes (Prestemon and Abt 2001). Harvest rates are heavily influenced by volatile wood product markets which feed into and are fed by overall economic activity as measured by GDP (Daniels 2005; Luppold and Miller 2005).

In the western stratum, the NAFD results show an early decrease and then significant increases, peaking in 2000. These dynamics likely relate to decreased western harvests in the early 1990s, increased forest fires, particularly in the interior west in the late 1990s (Daniels 2005; mtbs.gov), and increased insect activity (Meddens and others 2012) (Figure 8A). The changes in fire dynamics follow the widely recognized pattern of drier and warmer conditions, more frequent fires, and more intense insect outbreaks over the last two decades in the western US and Canada (Williams and others 2010; Westerling and others 2006; Kurz and others 2008).
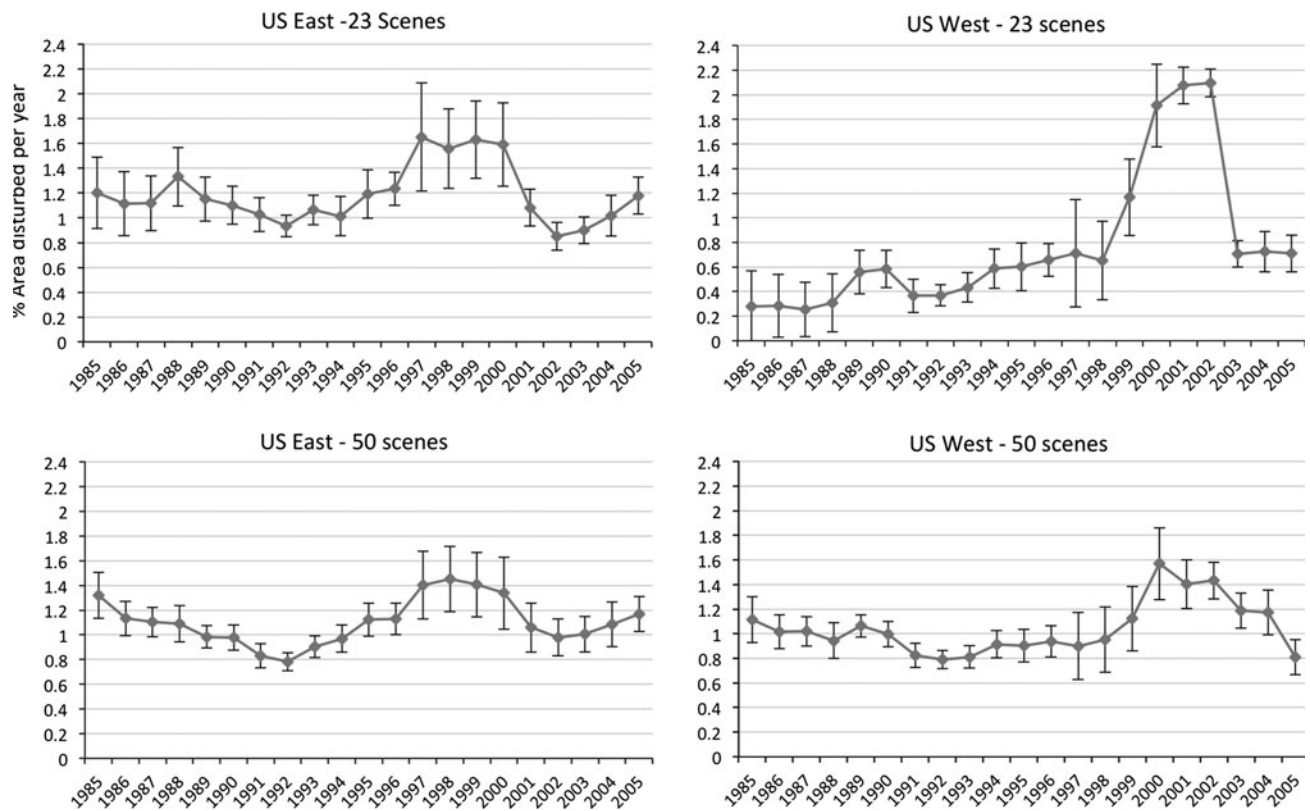
Figure 9. Comparison of phase I (23 scenes, *top*) and phase II (50 scenes, *bottom*) estimated disturbance rates (percent forest cover per year) and sampling error for the eastern (*left*) and western (*right*) strata.

In the eastern US, forest harvest appears to the dominant mechanism for disturbance, particularly is the southeastern US suggesting that these rates may be related to US economic activity as reflected in the gross domestic product (GPD) which strongly reflects changes in housing starts (Figure 8B) (Napton and others 2010). Recessions of 1990–1991 and 2000–2001 caused drops in the rate of increase of GDP that were mirrored by drops in eastern forest disturbance, and the period of highest disturbance rate (1997–2000) was also a period of large year over year increase in GDP.

Some caution must be exercised in interpreting these trends, however. A detailed analysis of the per-scene results indicates that much of the inter-annual variability in the eastern stratum was driven by accelerated harvest between 1996 and 2000 in two sample scenes in Oklahoma (WRS-2 p26r36) and eastern Texas (WRS-2 p26r37) (Schleeweis 2012). The sudden increase in harvest rates was noted at the time by the Assistant State Forester for Oklahoma (K. Atkinson, personal communication), and was attributed to a combination of regional timber prices, local increases in demand and capacity due to the opening of new chip and stud

mills, and real estate exchanges by timber companies.

Although the scene-level Landsat VCT products successfully captured this local acceleration in disturbance, such isolated (in space and time) jumps in disturbance rate were not built into the original sampling framework. Two of the drivers of the sampling scheme were the capture of a range of forest types (forest diversity) and the maximization of sample geographic dispersion. Essentially, the existence of isolated ''pockets'' of rapid disturbance, which could not have been predicted a priori and thus could not be incorporated into the sampling framework, raises questions as to the efficacy of using a limited geographic sample to fully capture variability in disturbance rates. Similar points have been made regarding tropical deforestation, which also exhibits a geographic ''clumping'' that is difficult to predict a priori (Tucker and Townshend 2000).

Sample Size and Sampling Error

The analysis of the 50-scene NAFD sample was conducted in two phases: a first phase using 23

scenes, and a subsequent phase with an additional 27 scenes. This gives us an opportunity to examine the effect of increased sample size on stratum-level estimates. Mean disturbance rate and variances were calculated separately for the samples from the first phase and the entire 50-scene set. Adding more scenes to the sample should improve the precision of the disturbance estimates, and the new rates should typically lie within two standard deviations of the estimates from the smaller set.

Comparing the phase 1 and combined phases 1 and 2 results (Figure 9) for the eastern stratum, the overall temporal pattern is similar, and the individual rates from the full set actually lie within the $1\,\sigma$ of the smaller set. However, in the western stratum, estimates of rates during particular eras (mid-1980s, 2000–2002) are separated by at least two standard deviations. Although it is reasonable to assume that the full set of 50 scenes provides a more precise estimate than the smaller phase 1 sample, this again illustrates the difficulty in using a limited geographic sample to capture regional disturbance rates.

CONCLUSIONS

The NAFD project has used a geographic sample of Landsat scenes to quantify forest disturbance rates across the conterminous United States for the 1985–2005 epoch. We found that an average of 2.77 Mha y^{-1} (1.09% forestland y^{-1}) was disturbed each year during this epoch. Adjusting this figure for the net measurement error (bias) would increase it to 3.63 Mha y^{-1} (1.42% forestland y^{-1}). Both of these figures are lower than the combined area affected by harvest, fire, and insect damage reported from land management inventories, although the figure is higher than the disturbance rate of forestland expected from the FIA age distribution. Much of the discrepancy is associated with low severity disturbances in which a small fraction of the canopy cover is killed.

Disturbance rates in the western US appear to have increased substantially beginning in the late 1990s and closely track increased fire frequency in the intermountain west during this period. Rates in the eastern US more closely tracked variability in economic activity (GDP), presumably reflecting fluctuations in harvest. The temporal variability in eastern disturbance was greater than expected, although it is unclear whether these variations reflect national patterns or local "pockets" of increased disturbance.

The work presented in this study points the way toward a consistent monitoring framework for US forest dynamics based on interannual satellite observations. Disturbance rates need to be quantified at the spatial resolution where human management and natural disturbances occur and at a time step relevant to driving processes. Although available forest inventories provide invaluable information on US forest dynamics, they have not been designed to provide a consistent geospatial view of disturbance. As a result, it is not clear from those data how long-term changes in land management and natural disturbance rates ultimately affect ecosystem structure and functioning across the nation. In principle, satellite observations can help meet this need.

The NAFD results described here relied on a limited geographic sampling, and the divergence in results between the initial set of 23 samples and the full set of 50 highlights the difficulty in using such a sampling approach to constrain disturbance dynamics. Our detailed analysis of the regional and local variations in the observed disturbance rates has revealed that the geography of processes that drive disturbance and specific local disturbance events have a strong influence over variations in area-averaged disturbance rates from year to year (Schleeweis 2012). As a result, we have turned toward wall-to-wall, annual mapping in the current phase of the NAFD project to circumvent these limitations. The advent of free Landsat data distribution, coupled with increased computing power, has led to the use of "every clear pixel" in mapping land dynamics (Zhu and others 2012). Availability of such comprehensive information will precipitate more advanced ecosystem process models that can ingest the richness of these data, and lead to a much improved ability to monitor and forecast ecosystem responses to climate change and human management. Coupled with repeat-measurement inventory data, when those become available over the next several years, we will likely soon have a powerful system for spatially explicit monitoring of forest cover in the conterminous US.

REFERENCES

Amiro BD, Barr AG, Barr JG, Black TA, Bracho R, Brown M, Chen J, Clark KL, Davis KJ, Desai AR, Dore S, Engel V, Fuentes JD, Goldstein AH, Goulden ML, Kolb TE, Lavigne MB, Law BE, Margolis HA, Martin T, McCaughey JH, Misson L, Montes-Helu M, Noormets A, Randerson JT, Starr G, Xiao J. 2010. Ecosystem carbon dioxide fluxes after disturbance in forests of North America. J Geophys Res 115:G00K02.

Birdsey R, Bates N, Behrenfeld M, Davis K, Doney SC, Feely R, Hansell D, Heath LS, Kasischke ES, Kheshgi H, Law B, Lee C, McGuire AD, Raymond P, Tucker CJ. 2009. Carbon cycle observations: gaps threaten climate mitigation policies. EOS Trans Am Geophys Union 90:292–3.

Böttcher H, Kurz WA, Freibauer A. 2008. Accounting of forest carbon sinks and sources under a future climate protocol—factoring out past disturbance and management effects on age-class structure. Environ Sci Policy 11:669–86.

Bucha T, Stibig HJ. 2008. Analysis of MODIS imagery for detection of clear cuts in the boreal forest in north-west Russia. Remote Sens Environ 112:2416–29.

Cochran WG. 1977. Sampling techniques. 3rd edn. New York: Wiley.

Cohen WB, Spies T, Alig RJ, Oetter DR, Maiersperger TK, Fiorella M. 2002. Characterizing 23 years (1972–95) of stand replacement disturbance in western Oregon forests with Landsat imagery. Ecosystems 5:122–37.

Cohen WB, Zhiqiang Y, Kennedy RE. 2010. Detecting trends in forest disturbance and recovery using yearly landsat time series: 2. TimeSync—tools for calibration and validation. Remote Sens Environ 114:2911–24.

Daniels JM. 2005. The rise and fall of the Pacific Northwest log export market. General Technical Report PNW-GTR-624. USDA, Forest Service, Pacific Northwest Research Station, Portland, OR, 80 pp.

Drummond MA, Loveland TR. 2010. Land-use pressure and a transition to forest-cover loss in the eastern United States. Bioscience 60:286–98.

Eidenshink J, Schwind B, Brewer K, Zhu Z, Quatle B, Howard S. 2007. A project for monitoring trends in burn severity. Fire Ecol 3(1):3–21.

Frolking S, Palace MW, Clark DB, Chambers JQ, Shugart HH, Hurtt GC. 2009. Forest disturbance and recovery: a general review in the context of spaceborne remote sensing of impacts on aboveground biomass and canopy structure. J Geophys Res 114:G00E02.

Gallego FJ. 2005. Stratified sampling of satellite images with a systematic grid of points. ISPRS J Photogramm Remote Sens 59:369–76.

Gardner TA, Barlow J, Chazdon R, Ewers RM, Harvey CA, Peres CA, Sodhi NS. 2009. Prospects for tropical forest biodiversity in a human-modified world. Ecol Lett 12:561–82.

Goward SN, Masek JG, Cohen WB, Moisen G, Collatz GJ, Healey S, Houghton RA, Huang C, Kennedy R, Law B, Powell S, Turner D, Wulder MA. 2008. Forest disturbance and North American carbon flux. EOS Trans 89(11):105–6.

Hansen MC, Stehman SV, Potapov PV. 2010. Quantification of global gross forest cover loss. Proc Natl Acad Sci USA 107:8650–5.

He HS, Mlandenoff DJ. 1999. Spatially explicit and stochastic simulation of forest landscape fire disturbance and succession. Ecology 80:81–99.

Horvitz DG, Thompson DJ. 1952. A generalization of sampling without replacement from a finite universe. J Am Stat Assoc 47:663–85.

Howard JL. 2007. US timber production, trade, consumption, and price statistics 1965 to 2005. Research Paper FPL-RP-637, USDA Forest Service, Forest Products Laboratory, Madison, WI.

Huang C, Goward SN, Masek JG, Gao F, Vermote EF, Thomas N, Schleeweis K, Kennedy RE, Zhu Z, Eidenshink JC, Townshend JRG. 2009. Development of time series stacks of Landsat imagery for reconstructing forest disturbance history. Int J Digit Earth 2:195–218.

Huang C, Goward SN, Masek JG, Thomas N, Zhu Z, Vogelmann JE. 2010a. An automated approach for reconstructing recent forest disturbance history using dense Landsat time series stacks. Remote Sens Environ 114:183–98.

Huang C, Thomas N, Goward SN, Masek J, Zhu Z, Townshend J, Volegmann JE. 2010b. Automated masking of cloud and cloud shadow for forest change analysis. Int J Remote Sens 31:5449–64.

Johnson EW, Wittwer D. 2008. Aerial detection surveys in the United States. Aust For 71:212–15.

Kennedy RE, Yang Z, Cohen WB, Pfaff E, Braaten J, Nelson P. 2012. Spatial and temporal patterns of forest disturbance and regrowth within the area of the Northwest Forest Plan. Remote Sens Environ 122:117–33.

Knight JF, Lunetta RS. 2003. An experimental assessment of minimum mapping unit size. IEEE Trans Geosci Remote Sens 41:2132–4.

Kuemmerle T, Hostert P, Radeloff VC, Perzanowski K, Kruhlov I. 2007. Post-socialist forest disturbance in the Carpathian border region of Poland, Slovakia, and Ukraine. Ecol Appl 17:1279–95.

Kurz WA, Dymond CC, Stinson G, Rampley GJ, Neilson ET, Carroll AL, Ebata T, Safranyik L. 2008. Mountain pine beetle and forest carbon feedback to climate change. Nat Lett 452:987–90.

Lindenmayer DB, Franklin JF, Fischer J. 2006. General management principles and a checklist of strategies to guide forest biodiversity conservation. Biol Conserv 131:433–45.

Luppold WG, Miller GW. 2005. Influence of markets on the composition of Central Appalachian Forests. In: Alavalapati JRR, Carter DR, Eds. Competitiveness of southern forest products markets in a global economy: trends and predictions. Proceedings of the Southern Forest Economics Workshop 2004; 2004 March 14–16; St. Augustine, FL. School of Forest Resources Conservation, University of Florida, pp. 113–122.

Masek JG, Collatz GJ. 2006. Estimating forest carbon fluxes in a disturbed southeastern landscape: integration of remote sensing, forest inventory, and biogeochemical modeling. J Geophys Res 111(G01006), 15 pp.

Masek JG, Vermote EF, Saleous NE, Wolfe R, Hall FG, Huemmrich KF, Gao F, Kutler J, Lim TK. 2006. A Landsat surface reflectance dataset for North America, 1990–2000. Geosci Remote Sens Lett IEEE 3:68–72.

Masek JG, Huang CQ, Wolfe R, Cohen W, Hall F, Kutler J, Nelson P. 2008. North American forest disturbance mapped from a decadal Landsat record. Remote Sens Environ 112:2914–26.

McRoberts RE, Bechtold WA, Patterson PL, Scott CT, Reams GA. 2005. The enhanced forest inventory and analysis program of the USDA Forest Service: historical perspective and announcement of statistical documentation. J For 103:304–8.

Meddens AJH, Hicke JA, Ferguson CA. 2012. Spatiotemporal patterns of observed bark beetle-caused tree mortality in British Columbia and the western United States. Ecol Appl 22:1876–91.

Mildrexler DJ, Zhao M, Running SW. 2009. Testing a MODIS global disturbance index across North America. Remote Sens Environ 113:2103–17.

Miller DH. 1978. The factor of scale: ecosystem, landscape mosaic and region. In: Hammond KA, Macinko G, Fairchild WB, Eds. Sourcebook on the environment: a guide to the literature. Chicago: The University of Chicago Press. p 63–88.

Napton DE, Auch RF, Headley R, Taylor JL. 2010. Land changes and their driving forces in the Southeastern United States. Reg Environ Change 10(1):37–53.

Nepstad DC, Stickler CM, Soares-Filho B, Merry F. 2008. Interactions among Amazon land use, forests and climate: prospects for a near-term forest tipping point. Philos Trans R Soc Sect B 363:1737–46.

Potapov PV, Hansen MC, Stehman SV, Pittman K, Turubanova S. 2009. Gross forest cover loss in temperate forests: biome-wide monitoring results using MODIS and Landsat data. J Appl Remote Sens 3:033569.

Potter C, Tan PN, Kumar V, Kucharik C, Klooster S, Genovese V, Cohen W, Healey S. 2005. Recent history of large-scale ecosystem disturbances in North America derived from the AVHRR satellite record. Ecosystems 8:808–24.

Prestemon J, Abt R. 2001. Timber products supply and demand. In: Wear D, Greis J, Eds. Southern forest resource assessment. General Technical Report SRS-53, USDA Forest Service. Southern Research Station, Asheville, pp. 299–325.

Ruefenacht B, Finco MV, Nelson MD, Czaplewski R, Helmer EH, Blackard JA, Holden GR, Lister AJ, Salajanu D, Weyermann D, Winterberger K. 2008. Conterminous US and Alaska forest type mapping using forest inventory and analysis data. Photogramm Eng Remote Sens 74:1379–88.

Running SW. 2008. Ecosystem disturbance, carbon, and climate. Science 321:652–3.

Särndal C-E, Swensson B, Wretman J. 1992. Model assisted survey sampling. New York: Springer.

Schleeweis K. 2012. Towards a better understanding of forest change processes in the contiguous US. Department of Geographical Sciences. College Park: University of Maryland, p. 200.

Skole DL, Tucker CJ. 1993. Tropical deforestation and habitat fragmentation in the Amazon: satellite data from 1978 to 1988. Science 260:1905–10.

Smith WB, Miles PD, Perry CH, Pugh SA. 2009. Forest resources of the United States, 2007, Gen. Tech. Rep. WO-78. US Department of Agriculture Forest Service, Washington, DC, 336 pp.

Strahler AH, Woodcock CE, Smith JA. 1986. On the nature of models in remote sensing. Remote Sens Environ 20:121–39.

Thomas N, Huang C, Goward SN, Powell S, Rishmawi K, Schleeweis K, Hinds A. 2011. Validation of North American forest disturbance dynamics derived from Landsat time series stacks. Remote Sens Environ 115:19–32.

Townshend JRG, Huang C, Kalluri SNV, DeFries R, Liang S, Yang K. 2000. Beware of per-pixel characterization of land cover. Int J Remote Sens 21:839–43.

Tucker CJ, Townshend JRG. 2000. Strategies for monitoring tropical deforestation using satellite data. Int J Remote Sens 21:1461–71.

US Environmental Protection Agency. 2011. Inventory of US greenhouse gas emissions and sinks: 1990–2009 (EPA 430-R-11-005).

USCCSP. 2007. The first state of the carbon cycle report (SOCCR): the North American carbon budget and implications for the global carbon cycle. In: King A, Dilling L, Zimmerman GP, Fairman DM, Houghton RA, Marland G, Rose AZ, Wilbanks TJ, Eds. US Climate Change Science Program.

USDA Forest Service. 2010. Major forest insect and disease conditions in the United States: 2009 update. Technical Report FS-952. Washington, DC, 28 p.

Vermote EF, Tanre D, Deuze JL, Herman M, Morcrette JJ. 1997. Second simulation of the satellite signal in the solar spectrum, 6s: an overview. IEEE Trans Geosci Remote Sens 35:675–86.

Waring RH, Running SW. 2007. Forest ecosystems: analysis at multiple scales. 3rd edn. Amsterdam: Academic Press.

Westerling AL, Hidalgo HG, Cayan DR, Swetnam TW. 2006. Warming and earlier spring increases western US forest wildfire activity. Science 313:940–3.

Williams AP, Allen CD, Millar CI, Swetnam TW, Michaelsen J, Still CJ, Leavitt SW. 2010. Forest responses to increasing aridity and warmth in the southwestern United States. Proc Natl Acad Sci USA 107:21289–94.

Wofsy SC, Harris RC. 2002. The North American carbon program (NACP). Washington, DC: NACP Committee of the US Interagency Carbon Cycle Science Program, Global Change Research Program, p. 82.

Wulder MA, White JC, Cranny M, Hall RJ, Luther JE, Beaudoin A, Goodenough DG, Dechka JA. 2008. Monitoring Canada's forests. Part 1: completion of the EOSD land cover project. Can J Remote Sens 34:549–62.

Zhu Z, Woodcock CE, Olofsson P. 2012. Continuous monitoring of forest disturbance using all available Landsat imagery. Remote Sens Environ 122:75–91.